Struct Multidisc Optim (2015) 52:251–268
DOI 10.1007/s00158-015-1239-7

RESEARCH PAPER

The effect of ignoring dependence between failure modes on evaluating system reliability

Chanyoung Park[1] · **Nam H. Kim**[1] · **Raphael T. Haftka**[1]

Received: 25 August 2014 / Revised: 12 January 2015 / Accepted: 7 March 2015 / Published online: 13 April 2015

Abstract Assuming independence between failure modes makes system reliability calculation simple but it adds approximation error. Interestingly, error due to ignoring dependence can be negligible for a highly reliable system. This paper investigates the reasons and the factors affecting the error. Error in system probability of failure (PF) is small for high reliability when tail-dependence is not very strong or the ratio between individual PFs is large. We created various conditions using copulas and observed the effect of ignoring dependence. Two reliability-based design optimization problems with a 2-bar and a 10-bar trusses are presented to show the effect of error on the optimum design and the system PF calculation. For the 10-bar truss, there were 5 % error in system PF and mass penalty less than 0.1 % in the optimum design for a target system PF of 10^{-7} even though five truss failures were strongly correlated.

Keywords Multiple failure modes · Tail-dependence · System reliability · Dependence · Correlation · Reliability-based design optimization

1 Introduction

Evaluating system reliability has been recognized as an important step in reliability-based design optimization. Although many reliability analysis methods have been developed, calculating system reliability including dependence between failure modes is still considered as a challenging problem (Li et al. 2007).

Reliability analysis methods can largely be categorized into sampling-based methods (e.g., Monte Carlo Simulation (MCS), importance sampling and surrogate-based methods) and analytical methods (e.g., first-order reliability method and second-order reliability method).

MCS might be the best method to evaluate system PF, but it is computationally expensive to achieve an acceptable level of accuracy for high reliability, even with the use of importance sampling techniques to reduce the variance of MCS (Melchers 1989, 1999; Dey and Mahadevan 1998). To reduce computational cost in MCS, surrogate-based methods have been developed (Zheng and Das 2000). Sampling-based methods using surrogates can consider dependence between failure modes, but the computational cost of constructing surrogate models increases rapidly with dimensions, often called the curse of dimensionality (Ba-Abbad et al. 2006).

Since analytical methods are computationally efficient, they are computationally favorable for calculating reliability (Dey and Mahadevan 1998; Halder and Mahadevan 2000). However, they have difficulties in accounting for dependence between failure modes. Consequently, approximate approaches, such as the lower-upper bound method (Halder and Mahadevan 2000; Hohenbichler and Rackwitz 1983; Vanmarcke 1973) and probability network evaluation technique (PNET) method (Ang et al. 1975), have been developed.

However, it is not well known that the effect of dependence between failure events can weaken as PF decreases (Schmidt 2002). In other words, the effect of dependence between failure events can be negligible for highly reliable structural designs.

Often structures are required to be highly reliable (Elishakoff 2004). For example, the U.S. Army's introduction of a structural fatigue reliability criterion for rotorcraft has

✉ Nam H. Kim
nkim@ufl.edu

Chanyoung Park
cy.park@ufl.edu

Raphael T. Haftka
haftka@ufl.edu

[1] University of Florida, Gainesville, FL, USA

been interpreted as a requirement for component lifetime reliability of 0.999999 (Neal et al. 1992). With such a high magnitude of reliability, failures are extremely rare events. For such rare events, the effect of dependence between failure modes on system reliability can often be negligible.

It is well known that ignoring dependence between input uncertainties can result in large errors in calculating reliability (Melchers 1989). Consequently modeling and identifying dependence between input model uncertainty is an important issue (Noh 2009; Noh et al. 2010). However, surprisingly, ignoring dependence between failure modes, which is recognizable as dependence between output uncertainties, may not result in large errors in system reliability.

The objective of this paper is 1) to demonstrate that most cases the error due to ignoring dependence on system reliability can be small even with strong dependence between failure modes and 2) to explore conditions where even for high reliability, the error may not be small.

2 Dependence between failure modes and system probability of failure

Structural failure with multiple failure modes is modeled with uncertainties in limit states, which are also called output uncertainties. Therefore, dependence between failure modes is equivalent to dependence between output uncertainties. If there is a system with N failure modes, limit states are defined such that the i^{th} failure event occurs when

$$G_i \le 0, \quad \mathrm{i} = 1, \ldots, \mathrm{N} \tag{1}$$

while the system is intact when

$$G_i > 0. \tag{2}$$

The PF of a single failure mode is referred to as a marginal PF that is defined as

$$P_{f\,i} = \Pr(G_i \le 0) \tag{3}$$

Two commonly used concepts for multiple failure modes are a series and parallel failure models. In the series failure model, the system fails if any of its failure modes is activated. In the parallel model, the system fails if all of its failure modes are activated (Haldar and Mahadevan 2000). Therefore, the series failure model is the union of failures, while the parallel model is the intersection of failures. Both models are affected by dependence between failure modes.

In this paper, the effect of ignoring dependence is discussed with the series model, since the ways of approximating dependence for both series and parallel failure models are the same and the series model is a common failure scenario in structural design.

For example, the exact system PF of a series model composed of two failure modes is defined using the union of two limit states as

$$P_{f\,sys} = \Pr(\{G_1 \le 0\} \cup \{G_2 \le 0\}) \tag{4}$$

Using the well-known expansion theorem (Hohenbichler and Rackwitz 1983), the probability of the union of two events is decomposed as

$$P_{f\,sys} = \Pr(G_1 \le 0) + \Pr(G_2 \le 0) - \Pr(\{G_1 \le 0\} \cap \{G_2 \le 0\}) \tag{5}$$

Note that computational challenge occurs in calculating the last term on the right-hand side of (5), which requires integrating the joint PDF of two limit states. Approximate methods have been developed to evaluate the system PF without integrating the joint PDF over the failure region (Hohenbichler and Rackwitz 1983; Vanmarcke 1973; Ditlevsen 1979). However, if the two failure modes are assumed to be independent, then the calculation of system PF becomes straightforward because the last term in (5) becomes the product of marginal PFs. With the independence assumption, the system PF can be approximated by

$$P_{f\,sys}^{idp} = \Pr(G_1 \le 0) + \Pr(G_2 \le 0) - \Pr(G_1 \le 0)\Pr(G_2 \le 0) \tag{6}$$

where the superscript 'idp' represents the case with independence assumption. The main goal of this paper is to discuss the difference between (5) and (6).

2.1 Illustrative truss example

A simple two-member truss shown in Fig. 1 is used to illustrate the dependence between limit states. A horizontal force h and vertical force v are applied at the joint of two members. The truss structure has two failure modes due to the resulting stresses: failure of elements 1 and 2 when the corresponding stresses exceed the ultimate stress, σ_u, that the material can sustain. A_1 and A_2 are areas of elements 1 and 2, respectively.

The limit state and the member force of element 1 are defined as

$$\begin{aligned} G_1 &= A_1\sigma_{u1} - F_1 \\ F_1 &= \frac{1}{2}\left(\frac{v}{\cos\alpha} + \frac{h}{\sin\alpha}\right) \end{aligned} \tag{7}$$

The limit state and the member force of element 2 are defined as

$$\begin{aligned} G_2 &= A_2\sigma_{u2} - F_2 \\ F_2 &= \frac{1}{2}\left(\frac{v}{\cos\alpha} - \frac{h}{\sin\alpha}\right) \end{aligned} \tag{8}$$

It is assumed that the ultimate strength and two external forces are input uncertainties, and the height of the structure

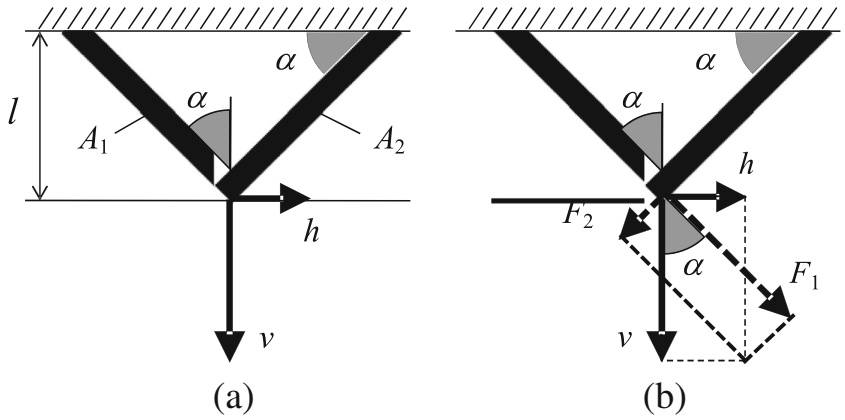

Fig. 1 A simple 2-bar truss in biaxial loading example

and angle are deterministic. The values and distributions of these variables is given in the reliability-based optimization example section. They lead to the two failure modes following a bivariate normal (BVN) distribution with a correlation coefficient of 0.8.

Figure 2a shows a scatter plot of 10,000 randomly generated limit state pairs, G_1 and G_2, which shows dependence between the two failure modes. The dependence between the failure modes is created by the angle between the structure and the external forces even if all input uncertainties are independent. The strength of dependence between G_1 and G_2, is 0.79 in terms of the linear correlation coefficient. Because the limit states are linear with respect to random variables and because these random variables are normally distributed, the joint probability density function (PDF) is bivariate normal distribution. The system PF, P_{fsys}, is estimated as the ratio of the number of samples in the shaded area in Fig. 2a to the total number of samples. The histograms shown on both axes are marginal histograms representing the marginal PDF of the limit states. Figure 2b is a contour plot of the joint PDF of the limit states based on the 10,000 samples.

3 Error in system reliability due to ignoring dependence

In this section, we investigate the effects of ignoring dependence on the error regarding three factors, the level of true system reliability, the correlation strength and the tail dependence. Examples were generated to examine the influences of the factors on the error. To regulate the influences of the factors, we chose a dependence model and set their parameters for each examples.

3.1 Error for bivariate normal distribution

It is easy to calculate the system PF if the two failure modes are assumed to be independent, but this incurs an error. Figure 3 shows the difference in intersection probability with and without considering dependence

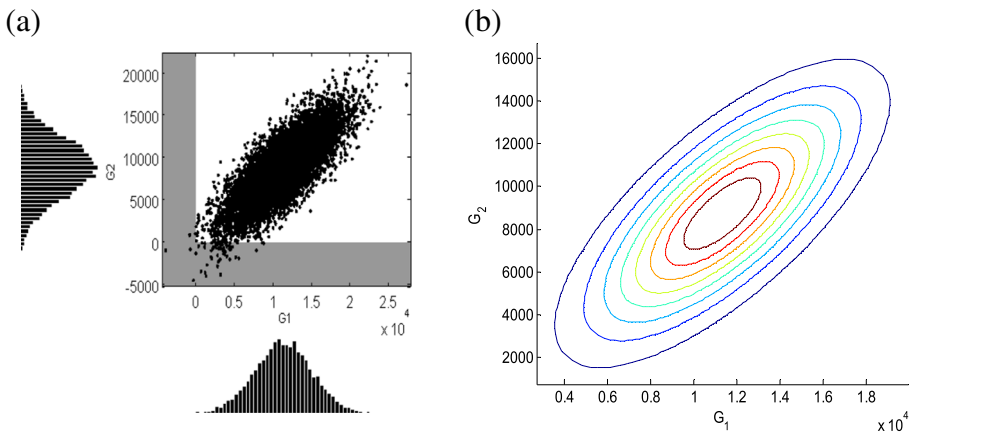

Scatter plot of random samples (shaded region is the failure region)

Contour plot of the joint PDF of G_1 and G_2

Fig. 2 Scatter plot of two limit states for 2-bar truss example. **a** Scatter plot of random samples (shaded region is the failure region). **b** Contour plot of the joint PDF of G_1 and G_2

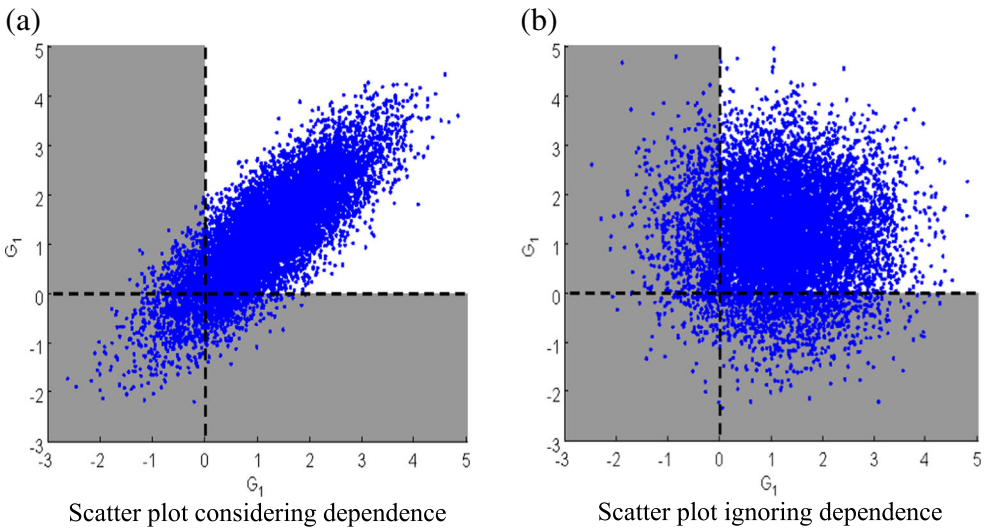

Fig. 3 Difference between intersection probabilities considering and ignoring dependence. **a** Scatter plot considering dependence $\begin{bmatrix} X_1 \\ X_2 \end{bmatrix} \sim N\left(\begin{bmatrix} 1.2 \\ 1.2 \end{bmatrix}, \begin{bmatrix} 1 & 0.8 \\ 0.8 & 1 \end{bmatrix} \right)$. **b** Scatter plot ignoring dependence $X_1 \sim N(1.2,1)$ and $X_2 \sim N(1.2,1)$

between two failure modes. Figure 3a shows 10,000 samples of the two dependent limit states. The samples are generated from bivariate normal distribution with mean vector of (1.2,1.2) and the standard deviation vector of (1.0,1.0), and a correlation coefficient of 0.8. The shaded region is the failure region and samples in the region represent failures. When the failure modes are assumed to be independent, the joint PDF is equal to the product of two marginal PDFs of limit states, whose corresponding samples are shown in Fig. 3b. The ratios of the numbers of failed samples to the total number of samples in different failure regions are shown in Table 1. The ratios include sampling errors due to the finite number of samples; the ratios in parenthesis are the true probability. It is noted that the standard error in each number in the table is approximately equal to its square root.

The percent error due to ignoring dependence is defined as

$$\text{Error} = \left| \frac{P_{f\,sys}^{idp}}{P_{f\,sys}} - 1 \right| \times 100(\%) \tag{9}$$

where $P_{f\,sys}$ is the system PF with dependence considered, while $P_{f\,sys}^{idp}$ is the probability assuming independence. The reliability index $\beta = -\Phi^{-1}(P_f)$ is another widely used measure, where $\Phi^{-1}(\bullet)$ is the inverse cumulative distribution function (CDF) of standard normal distribution. The percent error in terms of reliability index is defined as

$$\text{Error} = \left| \frac{\beta_{sys}^{idp}}{\beta_{sys}} - 1 \right| \times 100 = \left| \frac{-\Phi^{-1}\left(P_{f\,sys}^{idp}\right)}{-\Phi^{-1}\left(P_{f\,sys}\right)} - 1 \right| \times 100\,(\%) \tag{10}$$

where β_{sys}^{idp} is reliability index ignoring dependence and β_{sys} is the reliability index with dependence considered.

Table 1 Probability of failures in Fig. 3 (numbers in parenthesis are the numbers expected from the exact probabilities)

# of samples	Considering dependence	Ignoring dependence
$G_1<0$	0.1182 (0.1151)	0.1126 (0.1151)
$G_2<0$	0.1153 (0.1151)	0.1198 (0.1151)
$G_1<0$ and $G_2<0$	0.0679 (0.0665)	0.0138 (0.0132)
$G_1<0$ or $G_2<0$	0.1656 (0.1637)	0.2186 (0.2170)

3.2 The effects of magnitude of true system PF and the strength of dependence on error

In this section, an analytical example with two failure modes is used to study the effect of the true system PF level and the strength of dependence on error. The two failure modes are defined with a bivariate normal distribution (BVN). The system PF level and the strength of dependence are regulated by changing the mean and the linear correlation coefficient ρ, respectively.

Figure 4 illustrates four possible combinations of these two parameters and errors are different for difference cases. By evaluating errors for different true system PFs and different linear correlation coefficients, their effects can be discovered.

We make the two failure modes have the same marginal PFs, which is when the effect of dependence is strongest. The limit state functions are defined as

$$\begin{aligned} G_1 &= z - U_1\cos(45^\circ - \theta/2) - U_2\sin(45^\circ - \theta/2) \\ G_2 &= z - U_1\sin(45^\circ - \theta/2) - U_2\cos(45^\circ - \theta/2) \end{aligned} \tag{11}$$

where U_1 and U_2 are independent and follow the standard normal distribution, and θ is a parameter determining the correlation strength (unit of degree and maximal at $\theta=0^\circ$) and the

angle between the most probable points (MPPs) of the constraints. z is a parameter determining the level of reliability, with high values of z corresponding to low probability of failure.

Since the limit state functions are linear combinations of two independent normal random variables, the covariance matrix of the two limit states is easily derived as

$$\mathrm{cov}(G_1, G_2) = \begin{bmatrix} 1 & \sin(90^\circ - \theta) \\ \sin(90^\circ - \theta) & 1 \end{bmatrix} \tag{12}$$

In this case, the correlation matrix is identical to the covariance matrix. The joint PDF of limit states and parameters are then defined as

$$\begin{bmatrix} G_1 \\ G_2 \end{bmatrix} \sim N_2\left(\begin{bmatrix} z \\ z \end{bmatrix}, \begin{bmatrix} 1 & \rho \\ \rho & 1 \end{bmatrix} \right) \tag{13}$$

where $N_2(\bullet,\bullet)$ is BVN of G_1 and G_2 and $\rho = \sin(90^\circ - \theta)$.

Since the random variables U_1 and U_2 are standard normal and independent, the MPPs are found by plotting the limit state lines $G_1=0$ and $G_2=0$ as shown in Fig. 5. The minimum distance between the origin and the MPPs is the parameter, z. The angles between the limit state lines and U_1 and U_2 axis are θ. When the limit state lines are perpendicular, $\theta=90^\circ$, the linear correlation between two limit states is zero; that is, the two limit states are independent. When two limit state lines are aligned; i.e., $\theta=0^\circ$, the linear correlation coefficient becomes one, and the two MPPs overlap. In other words, when the two MPPs are very close, it implies that two failure modes are highly correlated.

Since the failure is associated with the negative region of limit states, the intersection probability of the two failures is obtained with cumulative distribution function (CDF) of the BVN. The exact system PF can be calculated with (5) and the system PF ignoring dependence is calculated from (6). The error is calculated with (9) and (10). The strength of dependence is usually categorized into four types: very weak ($0.0 \le \rho \le 0.4$), moderate ($0.4 \le \rho \le 0.7$), strong ($0.7 \le \rho \le 0.9$) or very strong ($0.9 \le \rho \le 1$) (Nelsen 1999). The error is calculated for strong correlation (0.7–0.9) in terms of the true system PF in the range of 10^{-1} to 10^{-6}.

The errors in reliability index and PF due to ignoring dependence are shown in Fig. 6 for different linear correlation coefficients, the magnitude of system PF and system reliability index. In general, the error is high when the level of true reliability index is low (or PF is large). In order to be more specific, Table 2 presents the required levels of system PF or reliability index to make the error less than target values. In Table 2, even with strong correlation, $\rho = 0.8$, the error in PF is less than 10 % for the true system PF of 10^{-4}, and the error in reliability index is less than 1 % for the true reliability index of 3.28. The observations imply that the effect of ignoring dependence becomes weak when PF is small.

One can observe from Table 2 and Fig. 6 that the error in system reliability index is much smaller than the error in PF. At this point, it is appropriate to note that at system low probabilities of failure, small errors in input distributions may lead to small errors in system reliability index but large errors in system PF. Therefore, striving for very accurate small system PF is out of reach for many cases. For example, a distribution of failure stress is typically estimated based on 100 test samples or less. The standard error of a standard deviation of a normal distribution based on 100 samples is 7 %. At a PF of 10^{-4}, this 7 % error would lead to approximately 7 % error in

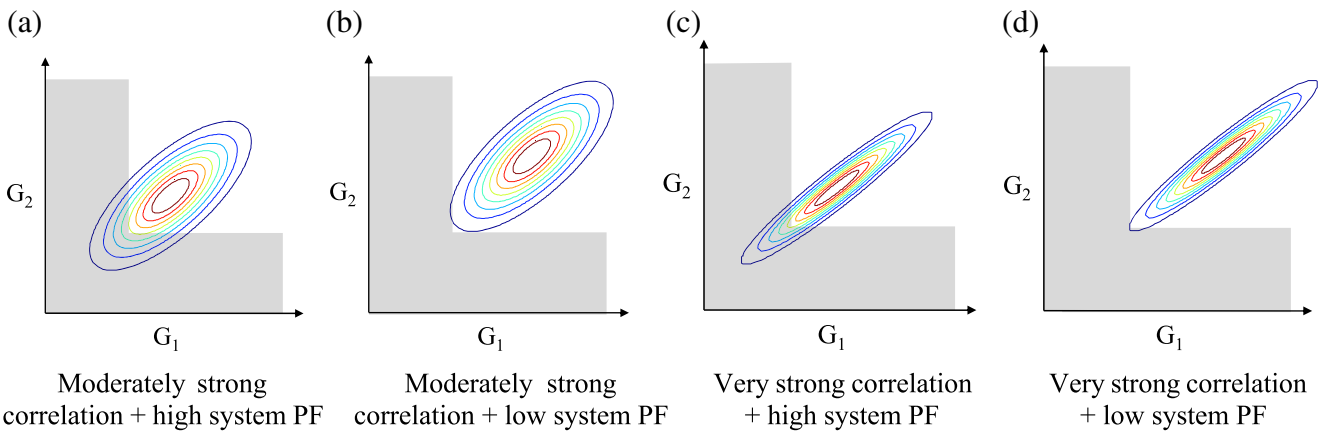

Fig. 4 Illustration of four cases regarding to the magnitude of the true system PF and the strength of correlation. **a** Moderately strong correlation+high system PF. **b** Moderately strong correlation+low system PF. **c** Very strong correlation+high system PF. **d** Very strong correlation+low system PF

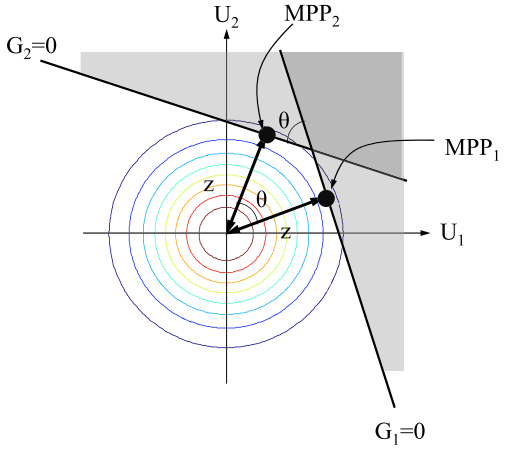

Fig. 5 Two correlated failure modes in the normalized space

reliability index, but more than 50 % error in PF. Therefore, a large relative error in PF is to be expected for a small PF from other reasons as well.

3.3 The effect of the degree of dependence in the tail on error

One way of estimating the dependence in the tail region is to check the shape of distribution. As shown in Fig. 3, independent distributions have circular-shaped contour at the failed tail region, while dependent distributions have a sharp contour in this region. For independent modes with a low PF, the low-left region of the contour is locally circular. On the other hand, if we had a distribution that is sharp in that region, as illustrated in Fig. 7b, it indicates that the tail-dependence is strong. The linear correlation coefficient is not sufficient to evaluate the level of dependence in the tail. The BVN shown in Fig. 7a has weaker dependence in the tail than the distribution shown in Fig. 7b even though they have the same linear correlation coefficient of 0.8.

For distributions with strong tail-dependence, we may expect that the error in PF decreases slowly, or will not decrease with decreasing PF. Thus, measuring the degree of tail-dependence is important, for which we rely on a statistical measure, denoted by L (Noh 2009; Venter 2002), for the lower tails of two distributions. The L function is the ratio between probability of intersection and marginal probability. When independence assumption is applied to the PF, it is the ratio between the probability of double failure and the probability of the first mode of failure (or the second since they are the same). More formally, the ratio is defined as a function of marginal PF as

$$L(z) = \Pr\left(\left\{G_1 \le \mathrm{F}_{G_1}^{-1}(z)\right\} \cap \left\{G_2 \le \mathrm{F}_{G_2}^{-1}(z)\right\}\right)/z \tag{14}$$

where z is the marginal probability, and $\mathrm{F}_{G_1}^{-1}(z)$ is the inverse CDF of G_1 for given probability z.

The reason that this ratio is relevant to our case is that the system PF is the sum of the two marginal probabilities of failure minus the probability of intersection (see 5). For independent limit states, $L(z)=z$ because the probability of the intersection is z^2 which is the square of the marginal probability when two marginal probability of failures are the same. However, for dependent limit states, the L function is away from $L(z)=z$ and the degree of discrepancy represents the degree of the dependence in the tail.

Figure 8a shows the degree of dependence in the tail of BVN as a function of marginal probability and the correlation coefficient. $L(z)=z$ for independent limit states. One can read an approximate error for different magnitudes of system PF from the figure. For example, when $z=10^{-5}$, the system PF is approximately 2×10^{-5}, and for $\rho=0.8$, we see that $L=0.14$, which estimates about a 7 % error in PF.

There are cases that the error does not decrease as the magnitude of system PF decreases because of strong tail-dependence. Figure 8b shows curves of L function for three different degrees of tail-dependence but with the same correlation coefficient. When an L function approaches the independent L function as z decreases, it represents that the effect of dependence is weakened in the tail. For strong tail dependence, however, L function remain constant and the effect of dependence remains strong in the tail.

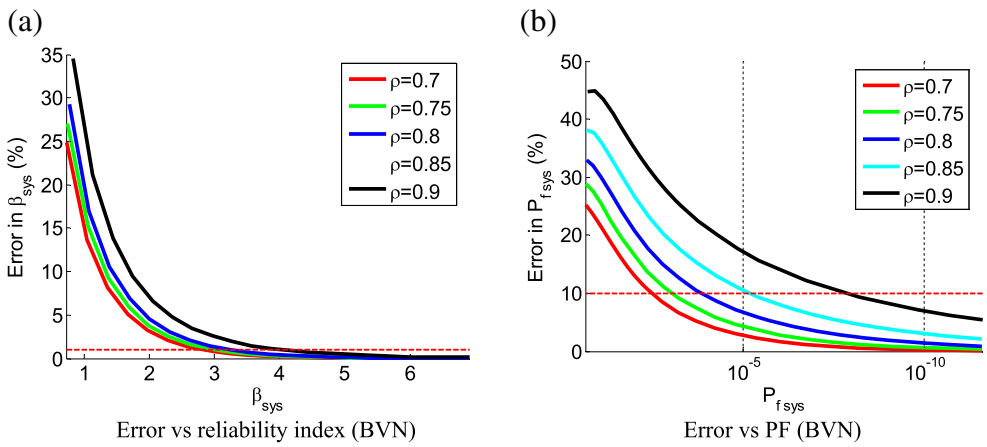

Fig. 6 The variation of error with magnitude of system PF for bivariate normal distribution with equal failure probabilities for the two modes. **a** Error vs reliability index (BVN). **b** Error vs PF (BVN)

Table 2 Minimum reliability index and maximum PF in order to achieve target errors

Reliability measure	Target error	ρ=0.7	ρ=0.75	ρ=0.8	ρ=0.85	ρ=0.9
Reliability index	5 %	1.68	1.79	1.93	2.10	2.31
	1 %	2.82	3.03	3.28	3.60	4.04
PF	10 %	3.4×10^{-3}	9.4×10^{-4}	1.4×10^{-4}	6.4×10^{-6}	1.6×10^{-8}
	5 %	1.7×10^{-4}	2.4×10^{-5}	1.4×10^{-6}	1.1×10^{-8}	1.5×10^{-11}

The red curve in Fig. 8b, a weak tail-dependence case, converges faster than that of BVN. The error of neglecting dependence is smaller than that of BVN for the same system PF and the error becomes negligible even for a relatively large system PF. However, the green curve in Fig. 8b, a strong tail-dependence case, does not decrease; error remains the same even for a very small system PF. The behavior of L function shows that the degree of dependence is very strong even in the extreme tail that there is almost no change in the L function.

Figure 9a shows the variation of error as a function of the magnitude of system PF for different tail-dependences. For a weak tail-dependence, even with a strong correlation coefficient, ρ=0.8, the error in PF is less than 10 % for the PF of 5×10^{-2} (blue curve). On the other hand, for a strong tail-dependence, the error stays high even for a low PF (green curve). In terms of the reliability index in Fig. 9b, even a strong tail-dependence does not change the trend of decreasing errors for high values of reliability index (low values of the PF).

The reason of different behaviors of errors in PF and reliability index is the nonlinear relationship between PF and reliability index. When PF=0.1, 10 % error in PF is equivalent to 5 % error in reliability index. When PF=0.01, however, 10 % error in PF yields 2 % error in reliability index. For the same error in PF, the equivalent error in reliability index decreases as PF decreases.

Table 3 presents the magnitudes of maximum system PF and minimum reliability index for different target errors. For example, for the weak tail-dependence, in terms of reliability index, there is only 1 % error when system reliability index is 1.98.

From Table 3, we can observe that for strong tail-dependence the error in system PF will not decrease, or decrease slowly with decreasing PF, while the error in reliability index will still decrease. A positive side is that the error in reliability index decreases even with strong tail-dependence as shown in Fig. 9b.

We use the L function as a measure of the degree of tail-dependence herein by estimating the tail-dependence coefficient (TDC) (Frahm et al. 2005). The limit of L is referred to as TDC that represents the strength of tail-dependence (Joe 1997).

$$\mathrm{TDC} = \lim_{z\to+0} L(z) \tag{15}$$

L for BVN converges to zero as z approaches zero; the error due to ignoring dependence decreases as system PF decreases. However, distributions with strong tail-dependence have non zero TDC. Unfortunately, accurate TDC estimation to determine the degree of tail-dependence requires more than 1,000 samples (Frahm et al. 2005).

4 Copula models

The previous sections BVN and generic strong and weak dependence models were used to generate examples. In this section, more dependence types will be used to enrich varieties in examples using copulas. The word ‘copula’ is a Latin noun which means ‘a link’. The word was employed in a statistical term by Sklar (Sklar 1959) in the theorem describing

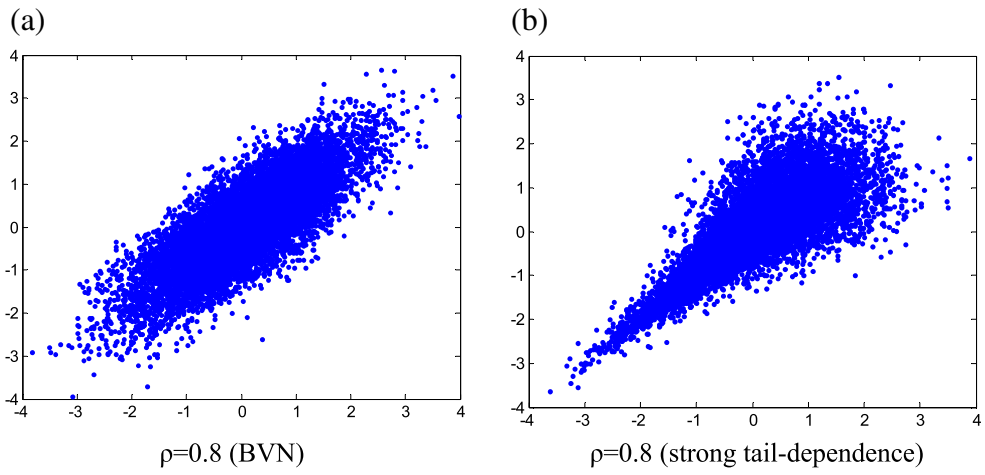

Fig. 7 Randomly generated 10,000 samples having different tail shapes with a linear correlation coefficient of 0.8. **a** ρ=0.8 (BVN). **b** ρ=0.8 (strong tail-dependence)

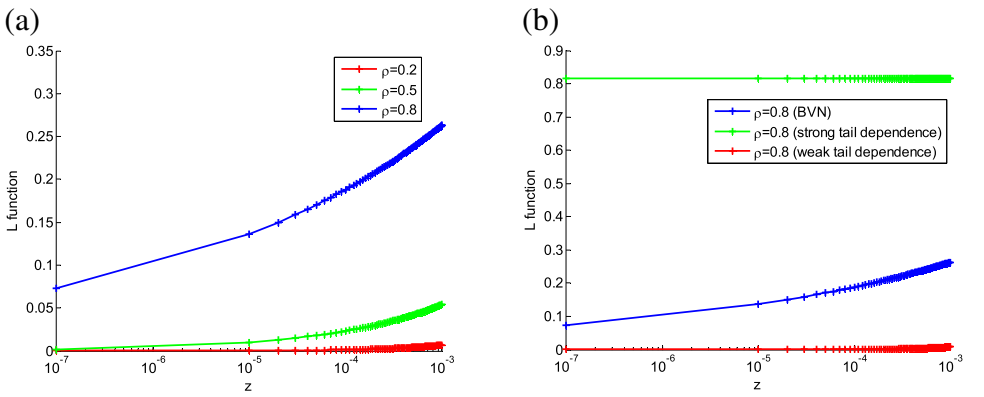

L function for different values of the strength of dependence (BVN)

L function for different magnitudes of tail-dependence

Fig. 8 Curves of *L* function with respect to the strength of dependence and tail shape of joint PDF. (Asymptotic value of *L*(z) for z→+0 is 0). **a** *L* function for different values of the strength of dependence (BVN). **b** *L* function for different magnitudes of tail-dependence

the functions that join marginal CDFs to form a joint CDF. In this context, copula is a function that links a joint CDF to its marginal CDFs (Nelsen 1999; Joe 1997; Georges et al. 2001). Copula is a joint CDF whose one-dimensional margins are uniform in the interval (0,1). Copula is an important concept for modeling a joint CDF that includes dependence.

However, defining complex multi-dimensional dependence is still a highly active area of research (Kurowicka and Joe 2011). Multivariate normal distribution (MVN) is one popular model to define multi-dimensional dependence, but it has a limitation that MVN can only model linear dependence of independent normal distributions. Also there are parameterized multivariate copulas, such as multivariate Clayton and multivariate Gumbel. For more general approaches, there are various approaches of non-copula based methods and copula-based methods. For copula-based methods, vine copula method is one of methods that modeling multi-dimensional dependence with flexibility based on well-established pair copulas families (Aas et al. 2009). Also there are graphical models based on directed acyclic graphs (Kurowicka and Joe 2011).

In this section, four common copulas in Fig. 10 are used to explain the tail-dependence and error in neglecting the dependence. It is noted that BVN is defined with Gaussian copula with normal marginal distributions, but the Gaussian copula is not limited to BVN. The marginal distributions of Gaussian copula can be any distribution. For example, we will observe the behavior associated with a Gaussian copula when the marginal distributions are Gumbel distributions.

Let $\mathbf{Y}=\{Y_1, Y_2, \ldots, Y_n\}^T$ be a vector of n-dimensional random variables, which are defined with marginal CDFs, $F_{Y_i}(y_i)$. The probability of intersection is a function of dependence. The probability of intersection of n-dimensional random variables is also called a joint CDF that is defined as

$$F_{Y_1,\ldots Y_n}(y_1,\ldots,y_n) = \Pr(Y_1 \le y_1, \ldots, Y_n \le y_n) \tag{16}$$

Copula functions define the joint CDF with marginal CDFs

$$F_{Y_1,\ldots Y_n}(y_1,\ldots,y_n) = C(F_{Y_1}(y_1),\ldots,F_{Y_n}(y_n)) \tag{17}$$

where C is a copula function. Note that copula functions are independent to marginal CDFs and all arguments of copula functions have a domain of [0, 1]. Also, due to the property of multivariate CDF, the output of the copula function also has a range of [0, 1].

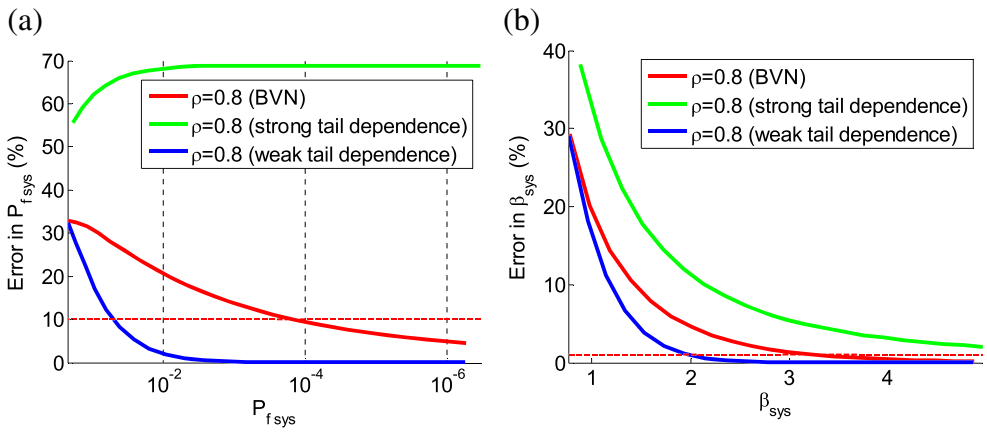

Error vs PF

Error vs reliability index

Fig. 9 Error curves for different strengths of tail-dependence. **a** Error vs PF. **b** Error vs reliability index

Table 3 Minimum reliability index and maximum PF needed for target error magnitudes

Reliability measure	Target error	ρ=0.8 (BVN)	ρ=0.8 (strong tail-dependence)	ρ=0.8 (weak tail-dependence)
Reliability index	5 %	1.93	3.13	1.44
	1 %	3.28	6.92	1.98
PF	10 %	1.4×10^{-4}	N/A	5.0×10^{-2}
	5 %	1.3×10^{-6}	N/A	2.5×10^{-2}

Figure 11 shows L function for the copulas shown in Fig. 10. As expected, the copula with a sharp tail, Clayton, has a very strong tail-dependence. Gaussian copula has stronger tail-dependence than Gumbel and Frank copulas.

It is noteworthy that the type of marginal distributions is immaterial as far as the error of ignoring dependence is concerned. The error is a function of the magnitude of system PF and the type of copula. For example, the error using a Gaussian copula with two lognormal marginal distributions will be the same as the error using the same Gaussian copula with BVN distributions. The readers are referred to Appendix A for a detailed explanation.

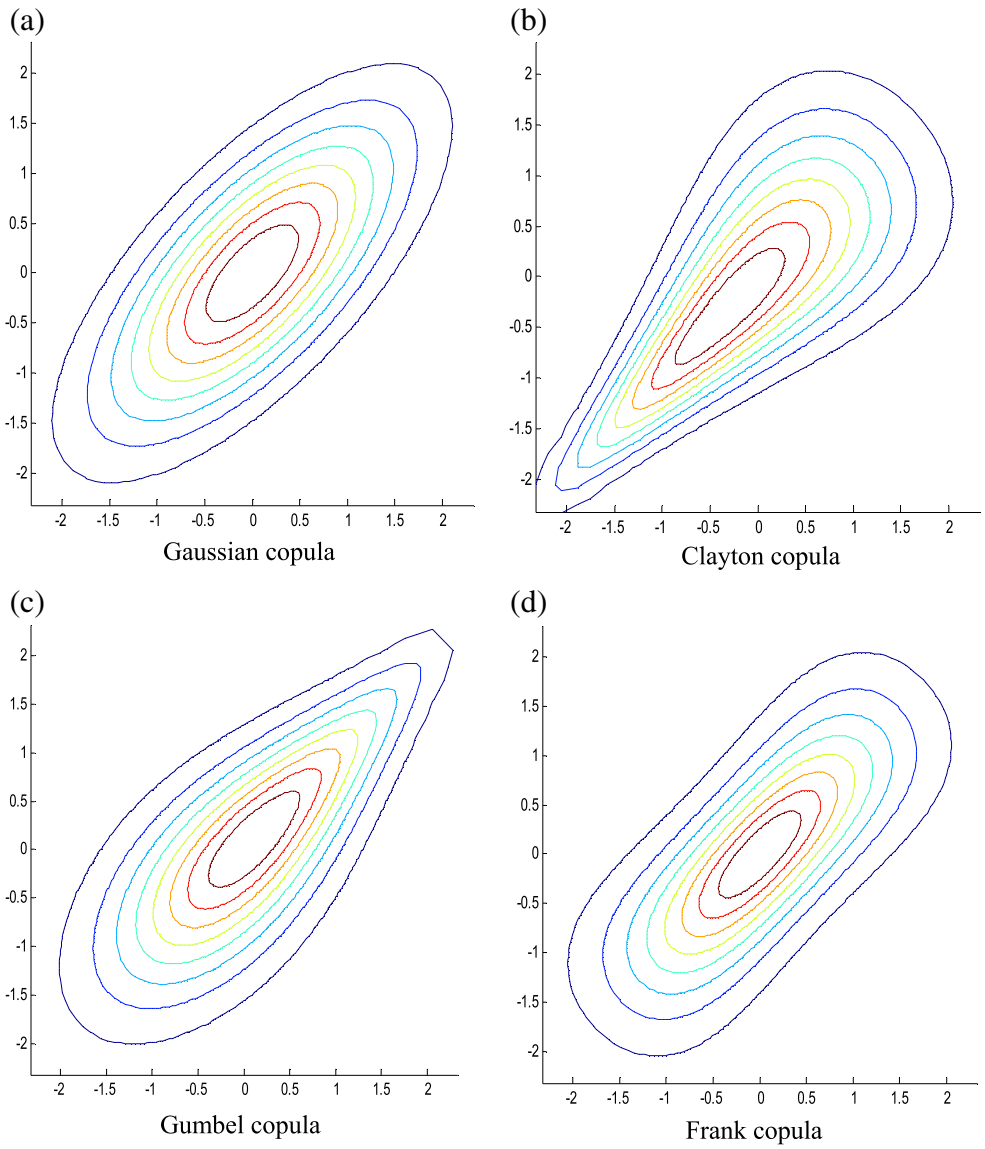

Fig. 10 Joint PDF shapes with four commonly used copulas with two standard normal marginal distributions with a linear correlation coefficient of 0.7. **a** Gaussian copula. **b** Clayton copula. **c** Gumbel copula. **d** Frank copula

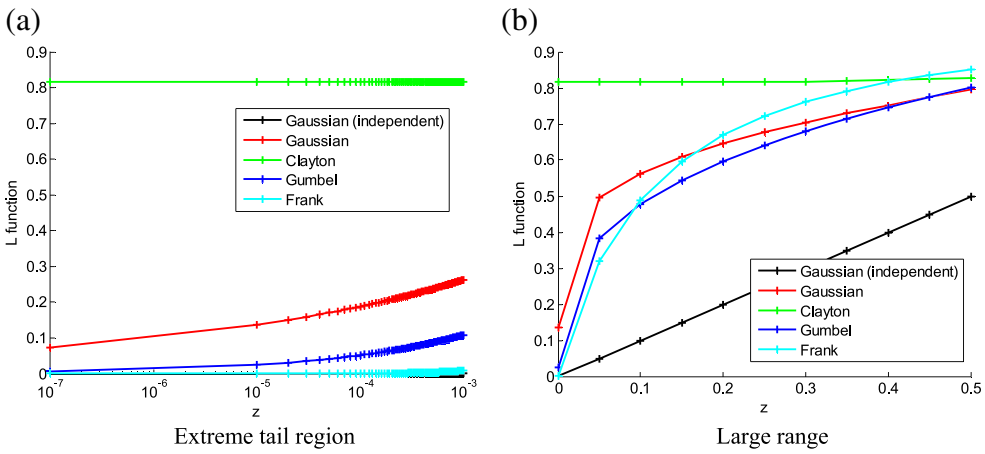

Fig. 11 L functions for different copulas. **a** Extreme tail region. **b** Large range

4.1 The effect of ignoring dependence for different copulas

In the previous section, the error due to ignoring dependence for BVN, which is defined with a Gaussian copula, is shown as a function of the magnitude of system PF and the correlation coefficient. In this section, the errors with different dependence models are defined with Clayton, Gumbel and Frank copulas. Since the type of marginal distributions are immaterial to the error (see Appendix A), the normal distributions are used as marginal CDFs. Then, the errors are calculated in terms of system PF and reliability index. The system PF shown in (5) is rewritten using a copula as

$$\begin{aligned} P_{f\,sys} &= F_{G_1}(0;z,1) + F_{G_2}(0;z,1) - C(F_{G_1}(0;z,1), F_{G_2}(0;z,1), \theta) \\ \beta_{sys} &= -\Phi^{-1}\left(P_{f\,sys}\right) \end{aligned} \tag{18}$$

The magnitude of PF and the strength of dependence are controlled by changing z and θ. PF ignoring dependence is expressed as

$$P_{f\,ind} = F_{G_1}(0;z,1) + F_{G_2}(0;z,1) - F_{G_1}(0;z,1)F_{G_2}(0;z,1) \tag{19}$$

The errors in (9) and (10) are shown in Fig. 12 for different correlation coefficients. It is observed that the error in system reliability index decreases as system reliability increases even for strong tail-dependence. In the case of system PF, however, the error does not decrease for the Clayton copula, but the error decreases for the other two copulas.

Although the Kendall's tau is used to define the level of dependence, the corresponding linear correlation coefficient is also shown for the purpose of consistency. For dependences defined with an elliptical joint distribution, Kendall's tau can be converted to the equivalent linear correlation coefficient with a formula of $\rho=\sin(0.5\pi\tau)$ (Lindskog 2000). For non-elliptical dependence, there is no universal way to convert Kendall's tau to the linear correlation coefficient. For example, the dependence between samples in Fig. 7a is defined with bivariate normal distribution, which is an elliptic joint pdf, whereas that in Fig. 7b is defined with a Clayton copula and two normal marginal distributions, which is a non-elliptic joint pdf. The strengths of dependence between two sample sets are 0.8 in terms of the linear correlation coefficient. However, in terms of the Kendall's tau, the strengths are 0.59 and 0.63, respectively. We generate 10,000 samples with a given level of Kendall's tau, from which the corresponding linear correlation coefficient is calculated. This process is repeated for different Kendall's tau to find the specific value of linear coefficient.

Table 4 presents the magnitudes of minimum system reliability indices for 5 and 1 % target errors. From Fig. 12 and Table 4, we see that, as expected, for the Frank and Gumbel copulas, which have weak tail-dependence, the errors in the reliability index decay fast for high reliability index. However, even for the Clayton copula with a strong tail-dependence, the error reduces relatively fast. Error in the reliability index converges to zero as the reliability index increases. In Table 5, the magnitudes of maximum system PFs for 10 and 5 % errors are shown. The errors in PF with Gumbel and Frank copulas decrease as reliability indices increase since they have a weak tail-dependence. For Frank copula, the error becomes less than 5 % at the magnitude of 10^{-3} even at the very large correlation coefficient of ρ=0.9. For the Clayton copula model, on the other hand, the error in PF increases as reliability increases due to its strong tail-dependence.

4.2 Effect of the ratio between marginal PFs

The ratio between marginal PFs also turns out to have a significant effect on the error. The Gaussian and Clayton copulas are considered since the other copulas have a small error because of their weak tail-dependence. The ratio between P_{f2} and P_{f1} is denoted as α as

$$P_{f2} = \alpha P_{f1} \tag{20}$$

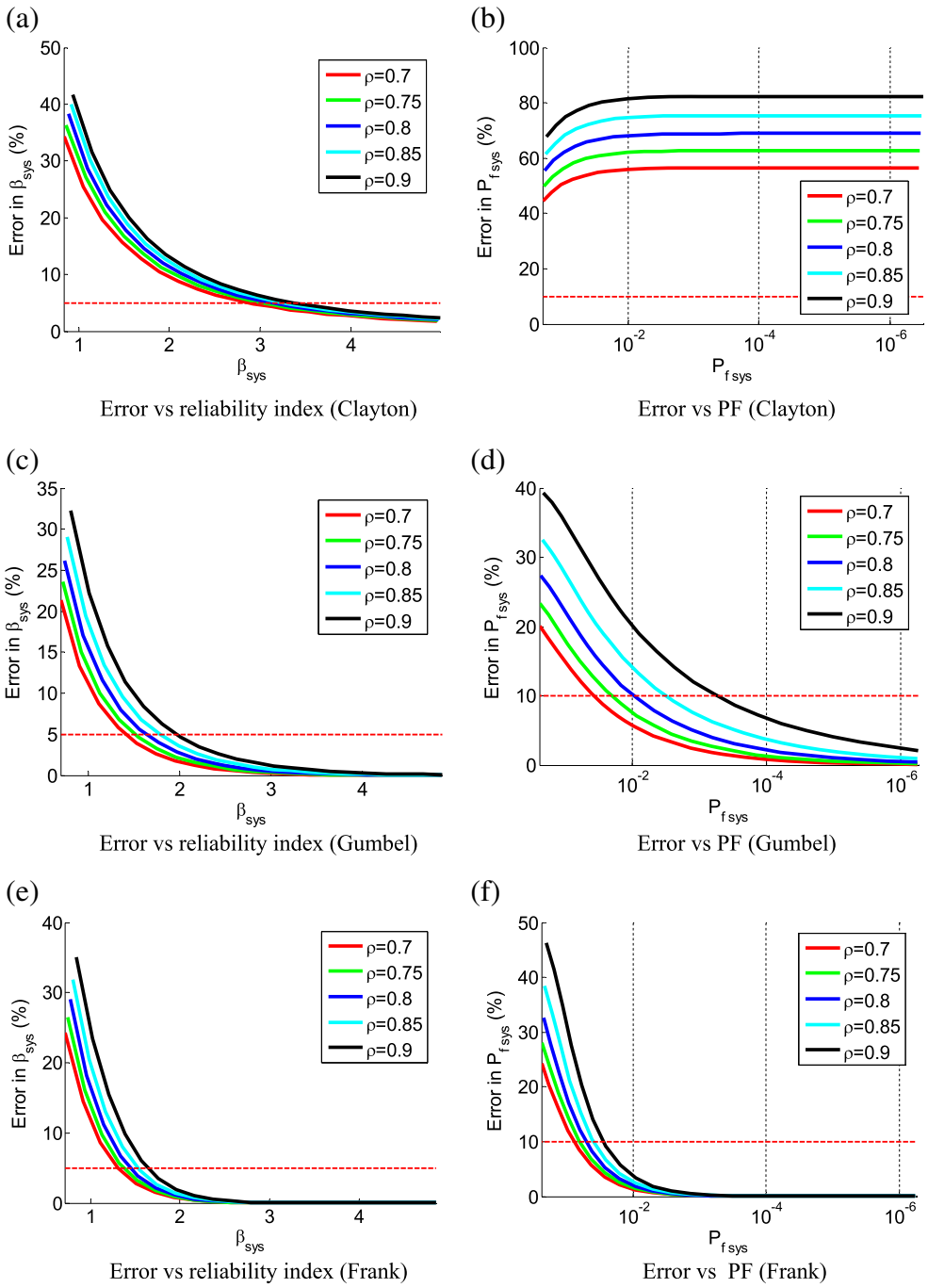

Fig. 12 Relative error in reliability index (*left figures*) and PF (*right figures*) versus system PF. **a** Error vs reliability index (Clayton). **b** Error vs PF (Clayton). **c** Error vs reliability index (Gumbel). **d** Error vs PF (Gumbel). **e** Error vs reliability index (Frank). **f** Error vs PF (Frank)

Figure 13 shows the error with respect to the magnitude of reliability index and logarithmic PF while the strength of dependence is kept as ρ=0.8. From the graphs, it is clear that the error is maximal when the ratio is 1 and decreases substantially with increasing ratio. For a strong tail-dependence copula, Clayton, the effect is most dramatic when the ratio is 8, even the errors in PF are near 10 %.

As the ratio increases, the error in reliability index and the error in PF decrease. Table 6 shows minimum reliability index for 5 and 1 % error with respect to the ratio of marginal PFs. The error monotonically decreases as reliability index increases. Table 7 shows maximum system PF for 10 and 5 % error with respect to the ratio. For Gaussian as a dependence model, the PF for 10 % error is 1.4×10^{-4} for the ratio of 1 and the PF for 10 % error is 1.7×10^{-4} for the ratio of 4. For the ratio of 8, the error is less than 10 % for all PF variation. For Clayton, the error is always larger than 10 % but the ratio of marginal PFs affects the error a lot as shown in Fig. 13d.

Table 4 Minimum system reliability index for 5 and 1 % target errors (in reliability index) versus the strength of dependence measured by the linear correlation coefficient

Copula	Target error \ ρ	ρ=0.7	ρ=0.75	ρ=0.8	ρ=0.85	ρ=0.9
Clayton	5 %	2.88	3.01	3.14	3.26	3.38
	1 %	6.50	6.72	6.92	7.10	7.27
Gumbel	5 %	1.40	1.50	1.63	1.78	1.96
	1 %	2.27	2.42	2.60	2.82	3.12
Frank	5 %	1.30	1.37	1.44	1.53	1.63
	1 %	1.86	1.92	1.98	2.06	2.17

5 Reliability based design examples

In this section RBDO for two truss structures, a two bar truss and a ten-bar plane truss, are carried out for different system reliability constraints to demonstrate the weakening effect on error in system PF calculation and the corresponding design mass penalty by ignoring dependence. For a given system reliability constraint, two optimum designs are obtained. One design is obtained by calculating system PF based on the independence assumption and the other without the assumption. For the design with the independence assumption, the corresponding true system PF is also evaluated. With n bars, the Optimization formulation is given as

$$\begin{aligned} \text{Minimize} \quad & Mass = \sum_{i=1}^{n} A_i L_i \rho \quad (kg) \\ \text{Subject to} \quad & \beta_{allow} < -\Phi^{-1}\left(P_{f_{sys}}\right) \\ & P_{f_{sys}} = \Pr\left(\bigcup_{i=1}^{n}\{G_i < 0\}\right) \\ & G_i = A_i\sigma_{u,i} - |N_i| \quad \text{for } i = 1,\ldots,n \\ & 0.01 \le A_i \le 1 \quad \text{for } i = 1,\ldots,n \end{aligned} \tag{21}$$

where A_i, L_i, N_i and $\sigma_{u,i}$ are the area, the length, the member force and the ultimate strength of i^{th} bar, respectively. The goal of the optimization is to obtain optimum areas for minimizing mass while satisfying system reliability constraint. It is assumed that the system is intact when all the bars are intact. A bar fails when the magnitude of an axial force exceeds its ultimate failure strength. In this section, in order to focus on measuring the effect of ignoring dependence and to make optimization process suitable, we use examples that have no errors in individual PF calculations with FORM.

5.1 Two-bar truss (n=2)

The previous truss structure in Fig. 1 is used for RBDO. The bar areas, A_1 and A_2, are design variables. FORM is used to evaluate marginal PFs during design optimization iterations and the system PF is calculated by assuming independence. Since the limit states are linear functions of normally distributed random variables, FORM provides the exact marginal PFs of two failure modes and the system PF can be exactly calculated through a simple algebra. The angle between the truss and the external loads v and h makes member forces, F_1 and F_2, dependent, which is defined with the Gaussian copula of the linear correlation coefficient 0.8. Consequently, the failure modes of the two members are also dependent. Table 8 shows input variables, as well as the distributions and the dependence model of the member forces F_1 and F_2.

Figure 14a shows the mass and the corresponding system reliability index as function of design variables. The dashed lines are contours of exact system reliability index (shown by the label) and the solid lines are contour lines with assumed independence. The discrepancy between the solid line and the dashed lines indicates mass penalty due to the error. It can be seen that for high values of A_1 or A_2 the discrepancy is very small. This is because the member with large area has low stress, so that only the failure mode in the other member is critical, and the dependence between failure modes has very little influence on the probability of failure. The filled 2D contour is mass, where light gray represents light mass and dark gray represents heavy mass. Optimum designs provide minimum mass for the specified system reliability index. The green star marker is the exact optimum design and the green circle marker is the optimum design ignoring dependence for target system reliability of β_{allow}=3.5.

Table 5 Maximum system PF for 10 and 5 % target errors in PF (not error in logarithm of PF) with respect to the strength of dependence measured by the linear correlation coefficient

Copula	Target error	ρ=0.7	ρ=0.75	ρ=0.8	ρ=0.85	ρ=0.9
Clayton	N/A[a]					
Gumbel	10 %	3.72×10^{-2}	2.07×10^{-2}	9.63×10^{-3}	3.21×10^{-3}	5.64×10^{-4}
	5 %	1.54×10^{-4}	4.79×10^{-5}	9.58×10^{-6}	8.52×10^{-7}	7.29×10^{-8}
Frank	10 %	7.7×10^{-2}	6.3×10^{-2}	5.0×10^{-2}	3.9×10^{-2}	2.7×10^{-2}
	5 %	7.3×10^{-3}	6.0×10^{-3}	4.9×10^{-3}	3.8×10^{-3}	2.7×10^{-3}

[a] Error for Clayton is always larger than 10 % for the magnitude of system PF less than 0.01

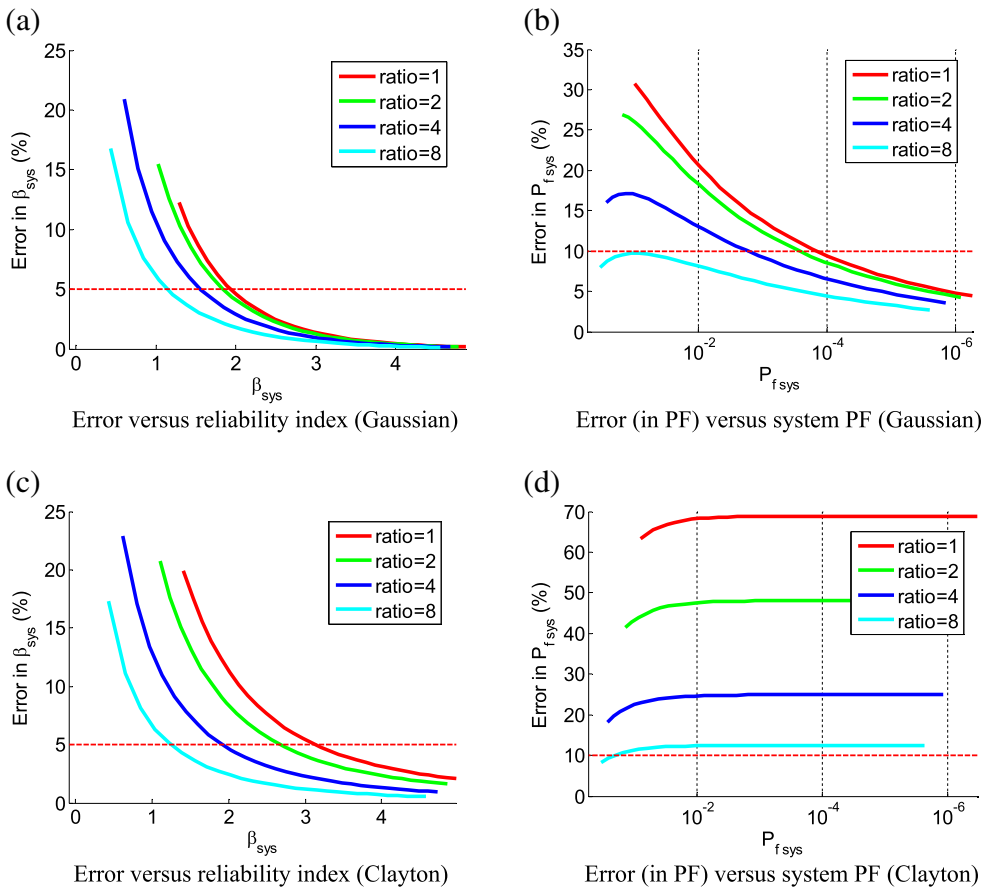

Fig. 13 The magnitude of errors for different ratios between marginal PFs. **a** Error versus reliability index (Gaussian). **b** Error (in PF) versus system PF (Gaussian). **c** Error versus reliability index (Clayton). **d** Error (in PF) versus system PF (Clayton)

For the allowable reliability index of 3.5, at the optimal design point, the dependence between the two failure modes is described with Gaussian copula and normal marginal distributions (BVN) with the linear correlation coefficient of 0.8 and the ratio between marginal probabilities of failure is 1.12 ($P_1=1.4\times10^{-4}$ and $P_2=1.2\times10^{-4}$).

Figure 14b presents three lines of mass versus required reliability index. The black solid line indicates the optimal design mass when dependence is ignored. The dashed line indicates the corresponding actual system reliability of that design, so that vertical difference between the two lines represents the reliability index error. For a design reliability index of 1.5 ($PF_{allow}=0.067$), the conservative error is 0.15 which translates to 36 % error in the probability of failure, while for a reliability index of 3.5 ($PF_{allow}=0.00023$) the error is 0.03 (or 12 % error in the probability). The errors in system PF and system reliability index are close to those presented in Fig. 6, in which the errors for a Gaussian copula dependence with the linear correlation coefficient of 0.8 and the ratio of 1 are presented.

The dashed line indicates the optimal design for given reliability constraint when dependence is exactly considered. The star and circle markers are the exact optimum design and the optimum design with independence assumption for $\beta_{allow}=3.5$, respectively. The mass

Table 6 Minimum system reliability index for 5 and 1 % target errors versus the marginal-probability ratio with $\rho=0.8$

Copula	Target error	ratio=1	ratio=2	ratio=4	ratio=8
Gaussian	5 %	1.94	1.84	1.56	1.14
	1 %	3.28	3.19	2.94	2.54
Clayton	5 %	3.14	2.68	1.92	1.25
	1 %	6.96	6.14	4.63	3.31

Table 7 Maximum system PF for 10 and 5 % target errors versus the marginal-probability ratio with $\rho=0.8$

Copula	Target error	ratio=1	ratio=2	ratio=4	ratio=8
Gaussian	10 %	1.4×10^{-4}	2.7×10^{-4}	1.7×10^{-3}	N/A[a]
	5 %	1.3×10^{-6}	2.5×10^{-6}	1.4×10^{-5}	2.9×10^{-4}
Clayton	N/A[b]				

[a] Error is always less than 10 %

[b] Error for Clayton is always larger than 10 % for the magnitude of system PF less than 0.01 when PF is smaller than 0.01

Table 8 Input variables for 2-bar truss design

Uncertainty variables	
Vertical force (v)[1]	$N(50, 15^2)$ kN
Horizontal force (h)[1]	$N(50, 2.5^2)$ kN
Ultimate strength (σ_{u1})[1]	$N(250, 12.5^2)$ Mpa
Ultimate strength (σ_{u2})[1]	$N(250, 12.5^2)$ Mpa
Calculated distribution of member forces	
Member force 1 (F_1)[2]	$N(70.71, 10.75^2)$ kN
Member force 2 (F_2)[2]	$N(0, 10.75^2)$ kN
Deterministic variables	
Angle (α)	45 (degree)
Height (l)	$0.5^{1/2}$ m
Density (ρ)	1 kg/m^3

[1] v, h, σ_{u1} and σ_{u2} are independent

[2] The member forces are dependent which is defined with a Gaussian copula with ρ=0.8

penalty is the additional mass of the optimal design mass ignoring dependence over the exact optimal design mass for the same system reliability constraint, so that horizontal distance between the solid and dashed lines is proportional to the mass penalty. There is 3.1 % mass penalty for β_{allow}=1.5 and the mass penalty is reduced to 0.5 % for β_{allow}=3.5. However, for this example the mass penalty provides additional design safety so that ignoring dependence does not harm the design safety.

For the previous example, the dependence between limit states is a Gaussian copula, which does not have strong tail-dependence. To create strong tail-dependence between failure modes, instead of defining distributions of the external forces, v and h, we artificially change the coupling between member forces F_1 and F_2 to the Gumbel copula with a strong coupling defined by Kendall's tau of 0.9 (see Table 9). Similarly those two ultimate strengths are coupled with Clayton copula. The forces and strengths have different copulas because they appear with opposite signs in the limit states (see also Fig. 10)

Figure 15 shows that strong tail-dependence leads to larger discrepancy between optimal designs for the same reliability constraint than the previous example. The star and circle markers are the exact optimum design and the optimum design with assumed independence, respectively. The error in system reliability index is 14 % for β_{allow}=1.5 and 2 % for β_{allow}=3.5. The corresponding errors in system PF are 64 and 35 %. There is 5.1 % mass penalty for β_{allow}=1.5 and 1 % for β_{allow}=3.5.

For the allowable reliability index of 3.5, at the optimal design point, the linear correlation coefficient between the two failure modes is 0.935. The ratio between marginal probabilities of failure is 1.12 ($P_1=1.4\times10^{-4}$ and $P_2=1.2\times10^{-4}$).

This example combines stronger linear correlation coefficient (0.935 vs. 0.8) and stronger tail-dependence (Gumbel and Clayton vs. all Gaussians). To separate the effects, we also ran a case where the linear correlation coefficient was 0.8 at the optimal design for β_{allow}=3.5 with the same strong tail-dependence. The error in system PF is 42 % for β_{allow}=1.5 and 30 % for β_{allow}=3.5. That is the strong tail-dependence had larger influence on the error in system PF calculation then the increase in linear correlation coefficient.

It is noteworthy that the strong correlation is due to the fact that randomness in the loads and strength affects the two failure modes in a similar way. That dependence does not mean that design improvement in one failure will affect the other failure. For this optimization problem, A_1

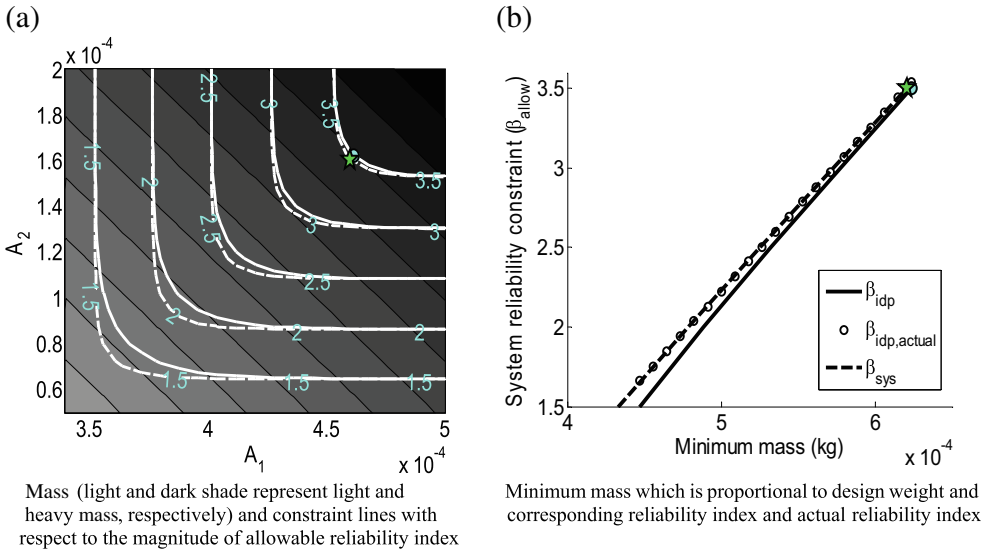

Fig. 14 Visualization of probabilistic optimization results (dashed lines show exact results, and solid lines results neglecting dependence) for 2-bar truss. (**a**) Mass (light and dark shade represent light and heavy mass, respectively) and constraint lines with respect to the magnitude of allowable reliability index. (**b**) Minimum mass which is proportional to design weight and corresponding reliability index and actual reliability index

Mass (light and dark shade represent light and heavy mass, respectively) and constraint lines with respect to the magnitude of allowable reliability index

Minimum mass which is proportional to design weight and corresponding reliability index and actual reliability index

Table 9 Random inputs for strong tail-dependence (the strength of dependence is defined with the Kendall's tau, τ) for 2-bar truss

Random inputs	Distribution
Member force 1 (F_1)[1]	$N(70.71, 10.75^2)$ kN
Member force 2 (F_2)[1]	$N(0, 10.75^2)$ kN
Ultimate strength (σ_{u1})[2]	$N(250, 12.5^2)$ MPa
Ultimate strength (σ_{u2})[2]	$N(250, 12.5^2)$ MPa

[1] F1 and F2 are dependent defined with a Gumbel copula with the Kendall's tan of 0.9

[2] σ_{u1} and σ_{u2} are dependent defined with a Clayton copula with the Kendall's tau of 0.9

will affect only the reliability of element 1 and A_2 will affect only the reliability of element 2.

5.2 Ten-bar plane truss example (n=10)

RBDO of a ten-bar plane truss shown in Fig. 16 is carried out. Cross-sectional areas of bars are design variables. Because the system is statically indeterminate, the axial force of a bar is a function of cross-sectional areas as well as the applied forces. Since member forces are linear combinations of the random applied forces, member forces N_i are correlated, and thus, the ten failure modes are correlated. The member forces in the bars are given by (Herencia et al. 2013)

$$
\begin{aligned}
&N_1 = P_2 - \frac{\sqrt{2}}{2}N_8; \quad N_2 = -\frac{\sqrt{2}}{2}N_{10}; \quad N_3 = -P_1 - 2P_2 - P_3 - \frac{\sqrt{2}}{2}N_8;\\
&N_4 = -P_2 - P_3 - \frac{\sqrt{2}}{2}N_{10}; N_5 = -P_2 - \frac{\sqrt{2}}{2}; N_8 - \frac{\sqrt{2}}{2}N_{10}; \quad N_6 = -\frac{\sqrt{2}}{2}N_{10};\\
&N_7 = \sqrt{2}(P_1 + P_2) + N_8; \quad N_8 = \frac{b_1 - a_{12}N_{10}}{a_{11}}; N_9 = \sqrt{2}P_2 + N_{10}; \quad N_{10} = \frac{b_2 a_{11} - b_1 a_{12}}{a_{11}a_{22} - a_{12}a_{21}}
\end{aligned}
\tag{22}
$$

where

$$
\begin{aligned}
a_{11} &= \left(\frac{1}{A_1E_1} + \frac{1}{A_3E_3} + \frac{1}{A_5E_5} + \frac{2\sqrt{2}}{A_7E_7} + \frac{2\sqrt{2}}{A_8E_8}\right)\frac{L}{2}; \quad a_{12} = a_{21} = \frac{L}{2A_5E_5}\\
a_{22} &= \left(\frac{1}{A_2E_2} + \frac{1}{A_4E_4} + \frac{1}{A_5E_5} + \frac{1}{A_6E_6} + \frac{2\sqrt{2}}{A_9E_9} + \frac{2\sqrt{2}}{A_{10}E_{10}}\right)\frac{L}{2}\\
b_1 &= \left(\frac{P_2}{A_1E_1} - \frac{P_1 + 2P_2 + P_3}{A_3E_3} - \frac{P_2}{A_5E_5} - \frac{2\sqrt{2}(P_1 + P_2)}{A_7E_7}\right)\frac{\sqrt{2}L}{2}\\
b_2 &= \left(-\frac{\sqrt{2}(P_3 + P_2)}{A_4E_4} - \frac{\sqrt{2}P_2}{A_5E_5} - \frac{4P_2}{A_9E_9}\right)\frac{L}{2}
\end{aligned}
\tag{23}
$$

Since the member forces are linear functions of applied forces, FORM provides the exact PF of each bar. Table 10 presents inputs and their definitions. The random input distributions were selected in order to create strong correlations between limit states.

Figure 17 shows the effect of ignoring dependence on the design mass and the error in system PF for different levels of reliability constraint. The optimum design mass with the independence assumption, β_{idp}, is different from the optimum design without using the assumption, β_{sys}. In Fig. 17, $\beta_{idp,actual}$

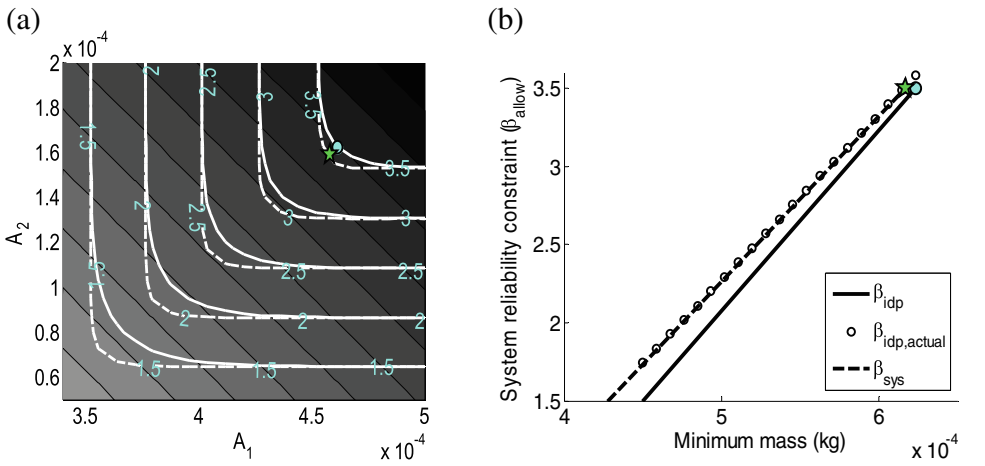

Fig. 15 Visualization of probabilistic optimization results with strong tail-dependence for 2-bar truss. (**a**) Mass (*bright* and *dark* color represent light and heavy mass, respectively) and constraint lines with respect to the magnitude of allowable reliability index. (**b**) Minimum mass which is proportional to design mass and corresponding reliability index and actual reliability index

Mass (bright and dark color represent light and heavy mass, respectively) and constraint lines with respect to the magnitude of allowable reliability index

Minimum mass which is proportional to design weight and corresponding reliability index and actual reliability index

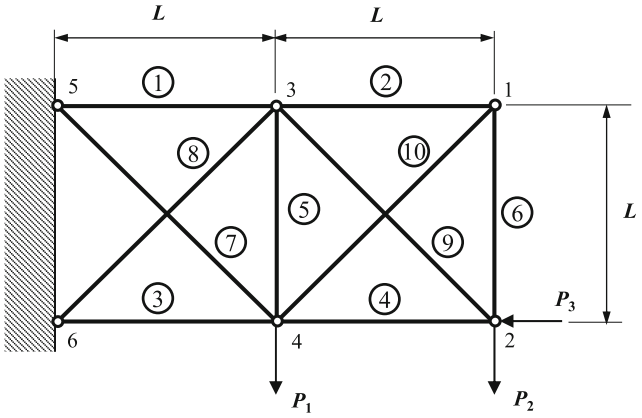

Fig. 16 Ten bar truss structure

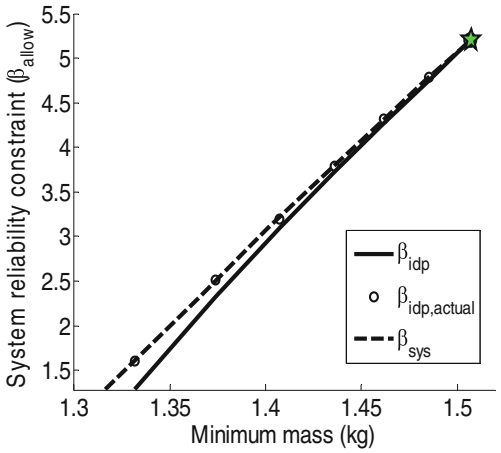

Fig. 17 Visualization of probabilistic optimization results

is the actual system reliability index corresponding to the optimum design obtained by β_{idp}. Because the design using β_{idp} underestimates the reliability, it yields a more conservative design than the design using β_{sys}. The error and the corresponding discrepancy of optimum mass decreases as the level of system reliability constraint increases. At $\beta_{allow}=1.28$ ($PF_{sys}=0.1$), the error in system reliability calculation is 45 % but the corresponding mass penalty is 1 %. This small mass penalty is caused by the small coefficients of variation of the applied forces and the ultimate strengths. At $\beta_{allow}=5.20$ ($PF_{sys}=10^{-7}$), the error in system reliability calculation is 5 % and mass penalty is less than 0.1 %.

The true system reliability indices of the design with independence assumption and the design without using the assumption were obtained by MCS. For calculating true system reliability indices, 10 million samples were used for $\beta_{allow}=1.28$ ($PF_{sys}=0.1$) to $\beta_{allow}=3.72$ ($PF_{sys}=10^{-4}$) and the number of samples increases as system reliability index increases to achieve the same level of accuracy. One hundred million, billion, ten billion samples were used for $\beta_{allow}=4.26$ ($PF_{sys}=10^{-5}$), $\beta_{allow}=4.75$ ($PF_{sys}=10^{-6}$) and $\beta_{allow}=5.20$ ($PF_{sys}=10^{-7}$), respectively. For obtaining the design without using the assumption, million samples were used for $\beta_{allow}=1.28$ ($PF_{sys}=0.1$) to $\beta_{allow}=3.09$ ($PF_{sys}=10^{-3}$) and the number of samples increases as system reliability index increase.

Table 10 Inputs and their definitions of the 10 bar truss (all random variables are independent)

Deterministic inputs	Value
Young's modulus (E_i) for i=1,..10	2.1 GPa
Density (ρ)	1 kg/m^3
Length (L)	1 m
Random inputs	**Distribution**
Applied forces (P_1)	$N(100, 5)$ kN
Applied forces (P_2)	$N(100, 5)$ kN
Applied forces (P_3)	$N(50, 2.5)$ kN
Ultimate strength ($\sigma_{u,i}$) for i=1,..10	$N(1,0.01^2)$ MPa

Randomness in PF calculation was suppressed during the optimization process by using a constant random seed.

Figure 18 presents correlations between limit states of bar 1, 2, 3, 5, 8 and 10 for $\beta_{allow}=1.28$ ($PF_{sys}=0.1$) and $\beta_{allow}=5.20$ ($PF_{sys}=10^{-7}$) with scatter plots from 10,000 samples and the linear correlation coefficients. Since PFs of bar 4, 6, 7 and 9 are essentially zero, correlations with those bars have no influence on system PF calculation. For example, the image in (2, 1) position is a correlation plot between bars 1 and 2 and the number in (1, 2) position is the corresponding correlation coefficient. Red samples in the scatter plots represent failed samples. In general, correlations are strong as ten out of 15 correlations are greater than 0.7, which is the lower bound of strong correlation (Georges et al. 2001). Figure 18 also provides PF ratios between failure modes. The numbers in parenthesis are marginal PFs of the design using the independence assumption and the ratio can be calculated using the numbers. For example the PF ratio between limit states of bars 1 and 2 is 1.33. The marginal PFs of the design without using the assumption are less conservative since the independence assumption overestimates the system PF and PF ratios are similar.

The correlations slightly decrease as the allowed reliability index increases. Since the ultimate strengths are independent, the increase in the required reliability index increases the bar areas and the corresponding coefficient of variation of resistance ($A_i\sigma_{u,i}$) of the limit state functions. It also weakens the strength of correlation between the limit states. Since the coefficients of variation of the ultimate strengths are much smaller than that of the applied forces, the effect of increasing the allowed reliability index on correlation strength change is small as observed.

6 Concluding remarks

In this paper, the effect of assuming independence between failure modes on error in system PF and system reliability index calculations was studied. It was found that the effects

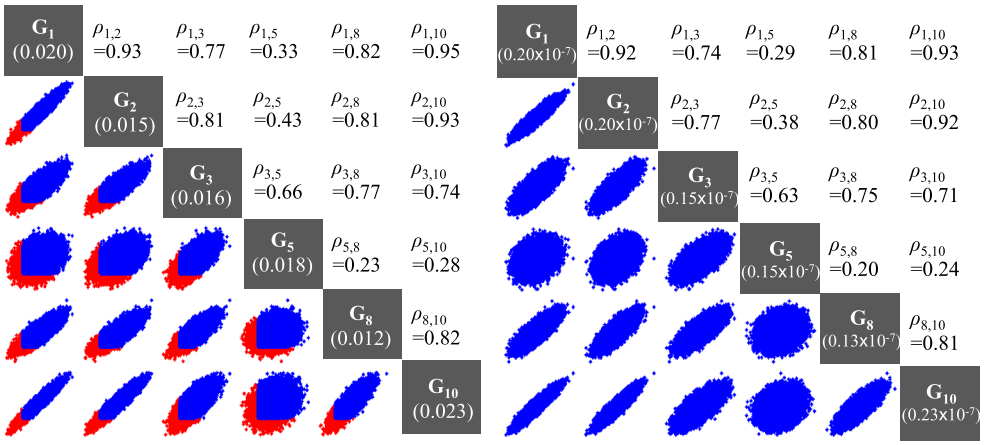

Fig. 18 Scatter plots of limit state correlations between bar 1, 2, 3, 5, 8 and 10 and the corresponding correlation coefficients for the optimal design of allowed system PF 0.1. (*Red* color of samples denotes failure)

of tail-dependence and the ratio between marginal PFs are significant. For low probabilities of failure, we can conclude that: 1) for errors in system reliability index, we can always ignore the dependence and 2) for errors in system PF, we can safely use independence assumption when the ratio of marginal PFs is high or tail-dependence is not very strong. In other words, we can determine whether errors in system PF is ignorable based on the ratio of marginal PFs and the tail-dependence. Note that there is no need to estimate the tail-dependence accurately. We can find out whether the tail strength is very strong by estimating the L function or TDC using MCS. For two failure modes, the conclusions are supported by the examples which are quite comprehensive but the examples are not sufficient to firmly support the conclusions for higher number of correlated failure modes. However, real applications have a lot of error sources, the error due to ignoring dependence would be likely be small compared to other error sources such as error in input distribution or error in computational models.

The bivariate normal distribution (BVN) and copulas were used to generate examples to demonstrate the effects of the correlation strength and tail-dependence. For the BVN with strong dependence with a correlation coefficient of ρ=0.8, there is 1 % error in the system reliability index at 3.28, and there is 10 % error in system PF at 10^{-4}. To illustrate the effect of tail-dependence, we used four commonly used copulas, Gaussian, Clayton, Gumbel and Frank copulas to generate examples. The decay of errors with increasing reliability index depends on a parameter called tail-dependence. For strong tail-dependence between failure modes, the errors in system PF do not decay even for a low system PF. Possibly, small errors in large values of reliability index are acceptable even if the relative errors in PF are high. This is because similar large errors in PF are inevitable due to small errors in input distributions.

It is also found that the ratio between marginal PFs is influential to the error, especially for strong tail-dependence. It is observed that the errors in PF are small when the ratio of marginal PFs is larger than 8 even for a strong tail-dependence.

Finally, examples of the design of a two-bar and ten-bar trusses were used to illustrate the effect of the error in reliability index on the optimum solution and the performance (here

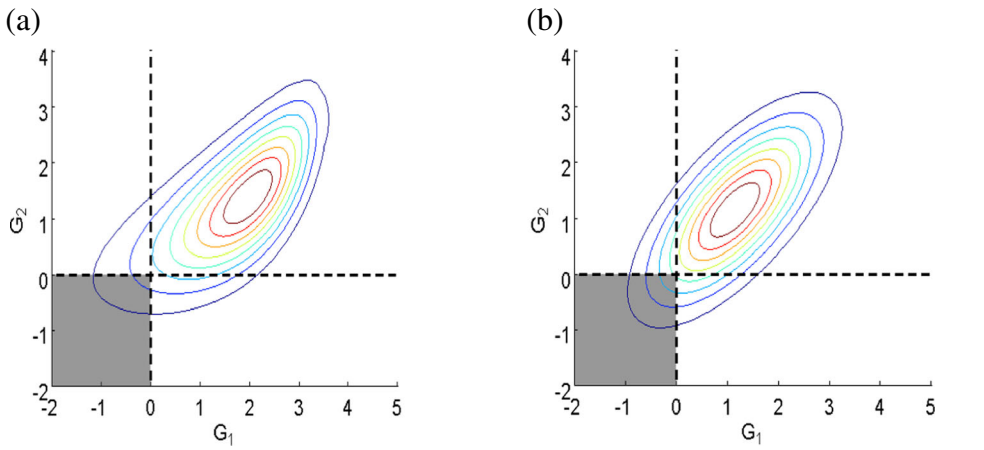

Fig. 19 Two joint PDFs that have different marginal PDFs for the limit states, but the same individual PFs

G_1 follows the extreme distribution with location parameter α=2 and scale parameter β=1. G_2 follows the normal distribution with mean μ=1.143 and standard deviation of σ=1; marginal PFs, G_1 and G_2, are the same $P_{f1} = P_{f2} = 0.1265$

G_1 and G_2 follow the normal distribution with mean μ=1.143 and standard deviation of σ=1; marginal PFs, G_1 and G_2, are the same $P_{f1} = P_{f2} = 0.1265$

design mass) penalty associated with it. For the two-bar example, it was found that even with very strong correlation (0.935) between two almost equally critical failure modes, at β_{allow}=3.5, the error in the reliability index was about 2 % and the mass penalty was only 1 %. For the ten-bar example, the error in the system PF of 45 % at β_{allow}=1.28 with strong dependences between bar failures decreases to 6 % at β_{allow}=5.20.

Acknowledgments This work was supported by the National Science Foundation, under the grant CMMI-0856431 by the U.S. Department of Energy, National Nuclear Security Administration, Advanced Simulation and Computing Program, as a Cooperative Agreement under the Predictive Science Academic Alliance Program, under Contract No. DE-NA0002378.

Appendix A: The effect of marginal distributions on the errors due to ignoring dependence

Since copula is independent to marginal distributions, error only depends on copulas. For example, two joint PDFs defined with same copula and different marginal PDFs have the same errors for the same marginal PFs. In other words, the types of marginal distributions do not affect the error.

Figure 19a and b show joint PDF contours of two failure modes. Figure 19a shows a joint PDF contour with different marginal distributions of limit state: the extreme distribution for G_1 and the normal distribution for G_2. Figure 19b shows a joint PDF contour with the same marginal distributions: the normal distribution for both G_1 and G_2. They have the same marginal PFs ($P_{f1} = P_{f2} = 0.1265$) and dependence model (the Gaussian copula with ρ=0.7). The shaded region is the region of intersection PF. Although the two joint PDFs have different contour shapes, their errors are the same, 19.8 %, since their marginal PFs and copula models modeling dependence are the same.

References

Aas K, Czado C, Frigessi A, Bakken H (2009) Pair-copula constructions of multiple dependence. Insurance: Math Econ 44(2):182–198

Ang AH, Chaker AA, Abdelnour J (1975) Analysis of activity networks under uncertainty. J Eng Mech Div 101(4):373–387

Ba-Abbad MA, Nikolaidis E, Kapania RK (2006) New approach for system reliability-based design optimization. AIAA J 44(5):1087–1096

Dey A, Mahadevan S (1998) Ductile structural system reliability analysis using adaptive importance sampling. Struct Saf 20(2):137–154

Ditlevsen O (1979) Narrow reliability bounds for structural systems. J Struct Mech 7(4):453–472

Eishakoff I (2004) Safety factors and reliability; friends or foes? Springer, New York

Frahm G, Junker M, Schmidt R (2005) Estimating the tail-dependence coefficient: properties and pitfalls. Insurance: Math Econ 37(1):80–100

Georges P, Lamy AG, Nicolas E, Quibel G, Roncalli T (2001) Multivariate survival modelling: a unified approach with copulas. Preprint from Groupe de Recherche Operationnelle, Credit Lyonnais

Haldar A, Mahadevan S (2000) Probability, reliability, and statistical methods in engineering design. Wiley, New York

Herencia JE, Haftka RT, Balabanov V (2013) Structural optimization of composite structures with limited number of element properties. Struct Multidiscip Optim 47(2):233–245

Hohenbichler M, Rackwitz R (1983) First-order concepts in system reliability. Struct Saf 1(3):177–188

Joe H (1997) Multivariate models and multivariate dependence concepts. CRC Press, Boca Raton

Kurowicka D, & Joe H (Eds.) (2011) Dependence Modeling: Vine Copula Handbook. World Scientific

Li J, Chen JB, Fan WL (2007) The equivalent extreme-value event and evaluation of the structural system reliability. Struct Saf 29(2):112–131

Lindskog F (2000) Linear correlation estimation. Preprint, ETH Zürich

Melchers RE (1989) Importance sampling in structural systems. Struct Saf 6(1):3–10

Melchers RE (1999) Structural reliability analysis and prediction. Wiley, New York

Neal DM, Matthews WT, Vangel MG, & Rudalevige T (1992) A Sensitivity Analysis on Component Reliability from Fatigue Life Computations, U.S. Army Materials Technology Laboratory MTL TR 92–5

Nelsen RB (1999) An introduction to copulas. Springer, New York

Noh Y (2009) Input model uncertainty and reliability-based design optimization with associated confidence level, Ph D. dissertation, Department of Mechanical Engineering, University of Iowa

Noh Y, Choi KK, Lee I (2010) Identification of marginal and joint CDFs using Bayesian method for RBDO. Struct Multidiscip Optim 40(1–6):35–51

Schmidt R (2002) Tail dependence for elliptically contoured distributions. Math Methods Oper Res 55(2):301–327

Sklar M (1959) Fonctions de répartition à n dimensions et leurs marges. Université Paris 8

Vanmarcke EH (1973) Matrix formulation of reliability analysis and reliability-based design. Comput Struct 3(4):757–770

Venter GG (2002) Tails of copulas. Proc Casualty Actuarial Soc 89(171):68–113

Zheng Y, Das PK (2000) Improved response surface method and its application to stiffened plate reliability analysis. Eng Struct 22(5):544–551